Fracture Mechanics of Concrete Structures
**Proceedings FRAMCOS-3**
AEDIFICATIO Publishers, D-79104 Freiburg, Germany

# NUMERICAL SIMULATION MODEL FOR MECHANICAL BEHAVIOR OF FIBER REINFORCED CONCRETE

T. Tsubaki
Department of Civil Engineering, Yokohama National University, Yokohama, Japan
S. Sumitro
Japan Structural Eng. and Computer Corp., Tokyo, Japan

**Abstract**
A numerical simulation model is presented for the analysis of the deformational behavior of fiber reinforced concrete. Microstructural unit elements are used to model the fiber reinforced concrete which is decomposed into fiber, matrix and interface between them. The nonlinear material properties are modeled separately for those three domains. The pullout behavior of parallel fibers at a crack surface is simulated taking into account the stiffness of the fiber.
Key words: Numerical simulation, fiber reinforced concrete, modeling

## 1 Introduction

Concrete is a composite material made up of coarse aggregate and mortar. The deformational behavior of concrete is nonlinear and influenced by the internal inhomogeneity. The effect of internal inhomogeneity is much more pronounced in case of fiber reinforced concrete. In order to understand the internal mechanism of such nonlinear deformational behavior including strain softening, it is necessary to consider an analysis method which can take into account the internal material structure of the size of aggregate.

Analytical models for the pullout behavior of fiber have been presented by Stang, *et al.*(1990) and Li, *et al.*(1991) for example. Those models are useful because the solution is given in a closed form which makes it easy to understand the overall behavior. A numerical simulation method is tried to be investigated in this study nevertheless because the nonlinear properties of material can be taken into account easily.

The analysis model considered in this study is called a microstructural unit element (see Tsubaki(1995)). It consists of two rigid blocks connected by nonlinear springs in the normal and tangential directions of the interface between rigid blocks. The mechanical behavior of fiber reinforced concrete is influenced by the local bond failure at the interface between the fiber and the matrix and the fiber rupture (see Fig.1(a)). If a proper size of microstructural unit elements is chosen to represent the domains for fiber, matrix and interface (see Fig.1(b)), then the pullout mechanism can be investigated taking into account the properties of fiber. In the following, the appropriateness of the present analysis model is examined through numerical simulation for the mechanical behavior of fiber reinforced concrete (see, e.g., Tsubaki and Sumitro(1997)).

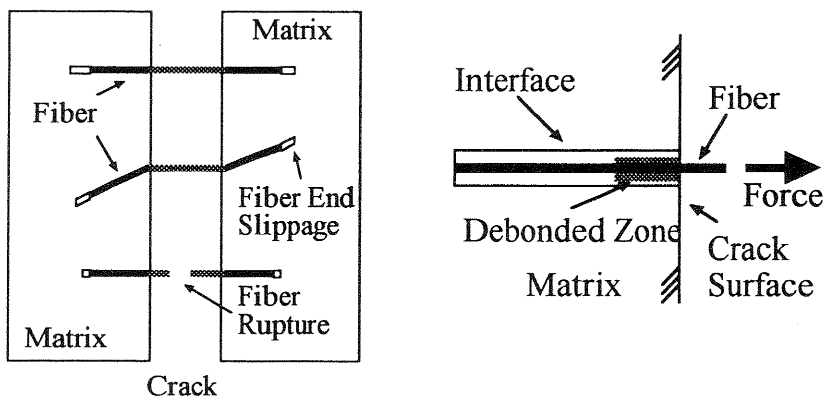


(a) Fiber at crack surface (b) Pullout mechanism

Fig.1. Pullout of fiber from matrix

## 2 Numerical simulation model

### 2.1 Microstructural unit element

The structure of a microstructural unit element is shown in Fig.2. It consists of two rigid blocks connected by two springs in the normal and tangential directions at the interface between rigid blocks. The mesoscopic inhomogeneous structure of a fiber reinforced concrete can be represented by microstructural unit elements by choosing appropriate element size considering the size of inhomogeneity. The incremental relationship between the surface tractions and the relative displacements in the normal and tangential directions of the interface between the rigid blocks of a microstructural unit element is expressed as follows.

$$\mathbf{k}\,d\mathbf{u} = d\mathbf{f};\ \ \mathbf{k} = \begin{bmatrix} k_n & 0 \\ 0 & k_t \end{bmatrix} \tag{1}$$

where $\mathbf{u} = [u_n, u_t]^T$ and $\mathbf{f} = [f_n, f_t]^T$ stand for the relative displacements and the surface tractions at the interface respectively. Subscripts $n$ and $t$ represent the normal and tangential directions of the interface between the rigid blocks. Matrix $\mathbf{k}$ stands for the properties of the springs in the normal and tangential directions.

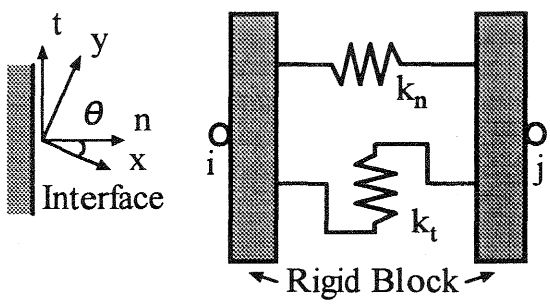


Fig.2. Microstructural unit element

## 2.2 Material modeling

The nonlinear material properties of component materials are modeled by properly assuming the matrix $\mathbf{k}$ which is a full matrix in general and is nonsymmetric in such a case as the phenomenon of friction or shear transfer. In the following analysis, it is assumed that $\mathbf{k}$ is diagonal as shown in Eq.(1). The material model is shown in Fig.3. The stiffness of the normal and tangential springs are reduced when the corresponding stress reaches the critical value. The number of stiffness reduction $N$ and the reduction ratio $\alpha$ are specified in the present study as follows: $N_t = 0$ for tension, $N_c = 3$ for compression, $N_s = 0$ for shear, and $\alpha = 0.5$ for all cases.

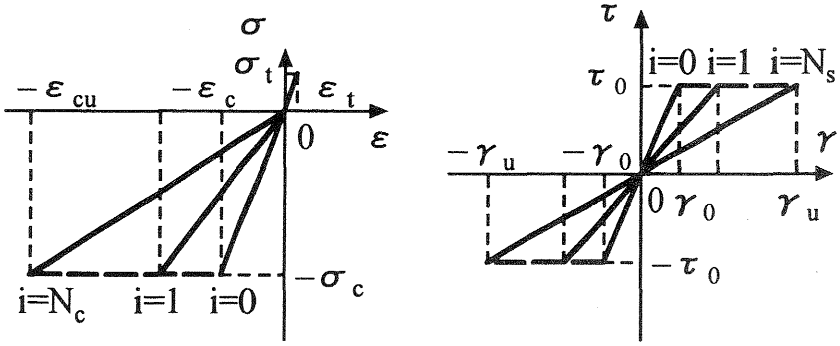


(a) Normal direction (b) Tangential direction

Fig.3. Material modeling

**2.3 Analysis method**

The numerical simulation is done by using the secant method to assure the numerical stability. The flow of calculation is summarized as follows.

1) Apply unit imposed displacement in the direction of the load for displacement control.
2) Solve the stiffness equation.
3) Calculate the normal and shear stresses at the element interface.
4) Find the element which first fails at the present loading stage.
5) Determine the actual imposed displacement from the ratio between the stress and the corresponding strength.
6) Reduce the stiffness of the failed spring by multiplying the reduction ratio $\alpha$.
7) Repeat these steps up to the global failure which is determined according to the excessively large value of the displacement.

If the global structure is considered to be made up of a number of similar small subdomains (see Fig.4), it is effective to use the domain decomposition method (see, e.g., Tsubaki(1991)). The stiffness equation for a subdomain is expressed in terms of the quantities related to internal nodes of the subdomain and those related to external nodes as follows.

$$\mathbf{K}d\mathbf{U} = d\mathbf{F};\ \ \mathbf{K} = \begin{bmatrix} \mathbf{K}_{II} & \mathbf{K}_{IE} \\ \mathbf{K}_{EI} & \mathbf{K}_{EE} \end{bmatrix};\ \ d\mathbf{U} = \begin{Bmatrix} d\mathbf{U}_I \\ d\mathbf{U}_E \end{Bmatrix};\ \ d\mathbf{F} = \begin{Bmatrix} d\mathbf{F}_I \\ d\mathbf{F}_E \end{Bmatrix} \tag{2}$$

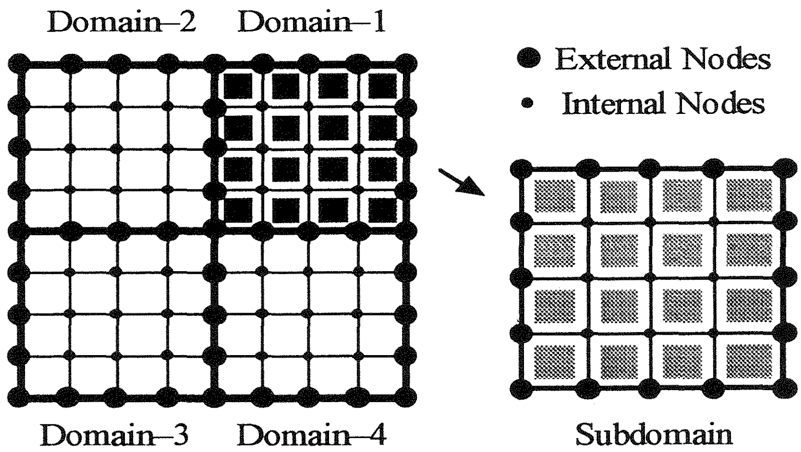


Fig.4. Domain decomposition method

where $\mathbf{K}$, $\mathbf{U}$ and $\mathbf{F}$ represent the stiffness matrix, the displacement vector and the load vector respectively for a subdomain. Subscripts $I$ and $E$ stand for quantities related to internal nodes and those related to external nodes of a subdomain respectively. Each part of partitioned stiffness matrix is decomposed by LD decomposition and the following relationships are obtained (see Adeli and Kamal(1992)).

$$\mathbf{K}_{II} = \mathbf{L}_{II}\mathbf{D}_{II}\mathbf{L}_{II}^T;\quad \mathbf{K}_{IE} = \mathbf{L}_{II}\mathbf{D}_{II}\mathbf{L}_{II}^T\mathbf{W}_{IE};\quad d\mathbf{F}_I = \mathbf{L}_{II}\mathbf{D}_{II}\mathbf{L}_{II}^T d\mathbf{V}_I \tag{3}$$

Eq.(3) defines $\mathbf{W}_{IE}$ and $d\mathbf{V}_I$. From Eq.(2) and Eq.(3), the displacement increments at internal nodes are obtained by the following equation.

$$d\mathbf{U}_I = d\mathbf{V}_I - \mathbf{W}_{IE}d\mathbf{U}_E \tag{4}$$

The stiffness equation for a subdomain is obtained by substituting Eq.(4) into Eq.(2) as follows.

$$\mathbf{K}^* d\mathbf{U}_E = d\mathbf{F}^* \tag{5}$$

$$\mathbf{K}^* = \mathbf{K}_{EE} - \mathbf{K}_{EI}\mathbf{W}_{IE} \tag{6}$$

$$dF^* = dF_E - K_{EI} dV_I \tag{7}$$

$K^*$ is the reduced stiffness matrix for the external nodal displacement increment $dU_E$, and $dF^*$ is the equivalent nodal force increment.

The overall domain can be analyzed from the global stiffness equation by assembling the stiffness equation of each subdomain under given displacement boundary conditions and load conditions. The internal stress is calculated after calculating the internal displacements. This domain decomposition method is effective in ordinary sequential computation as well as in parallel computation. The flow of analysis of the domain decomposition method is shown in Fig.5.

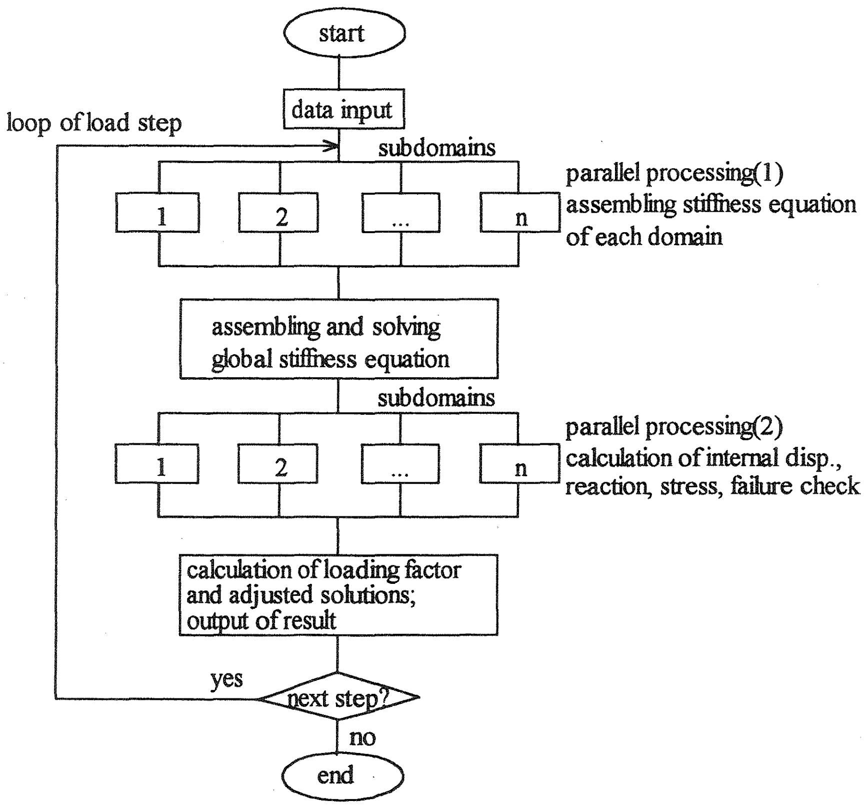


Fig.5. Flow of analysis with domain decomposition method

## 3 Numerical simulation of pullout of fibers

The pullout behavior of fibers at a crack surface is analyzed by using the above numerical simulation method. The size of the overall domain is $50 \times 100$mm. The overall domain is decomposed into five subdomains. Each subdomain contains one fiber (see Fig.6(a)). The fiber length is 32mm. The embedded length of fiber is 21mm for a long case and 11mm for a short case. There is a frictionless crack in the middle of the domain. The element discretization and the random distribution of element interface are shown in Fig.6(b,c). The number of nodes is 1326, and the number of elements is 2575. The fiber is modeled by connecting microstructural unit elements with an element interface whose normal direction coincides with the fiber direction. The interface zone between fiber and matrix is modeled by one layer of elements whose normal direction is perpendicular to the fiber (see Fig.6(b,c)). The element length is 2mm and the cross-sectional area used in the calculation of stress is set to be $2\text{mm}^2$.

The normal direction of the element interface is given by generating uniformly distributed random numbers between 45 and 135 degrees for a horizontal element and between –45 and 45 degrees for a vertical element.

The material constants are: $k_n = 3.3 \times 10^4$ N/mm, $k_t = 1.4 \times 10^4$ N/mm, $\sigma_c = 60\text{N/mm}^2$, $\sigma_t = 8\text{N/mm}^2$, $\tau_0 = 30\text{N/mm}^2$ for the matrix, $k_n = 3.3 \times 10^3$N/mm, $k_t = 8.0$N/mm, $\sigma_c = 30\text{N/mm}^2$, $\sigma_t = 3\text{N/mm}^2$, $\tau_0 = 4\text{N/mm}^2$ for the interface, and $k_n = 2.4 \times 10^4$ N/mm, $k_t = 2.4 \times 10^3$ N/mm for the stiff fiber. The spring constants of soft fiber are 1/100 of those of stiff fiber.

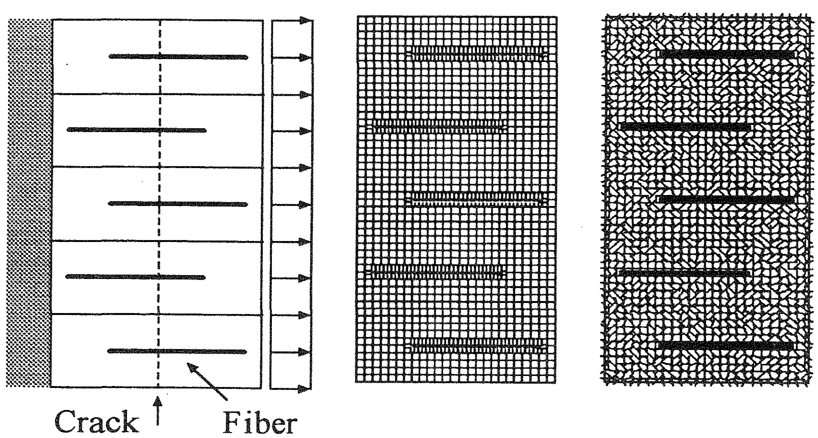


(a) Subdomains (b) Elements (c) Internal interfaces

Fig.6. Analysis of pullout of fiber

The fiber is assumed to be elastic. The initial material constants are uniformly given for all elements of each domain of matrix, fiber and interface. The statistical variation of the material is represented by the random orientation of the element interface.

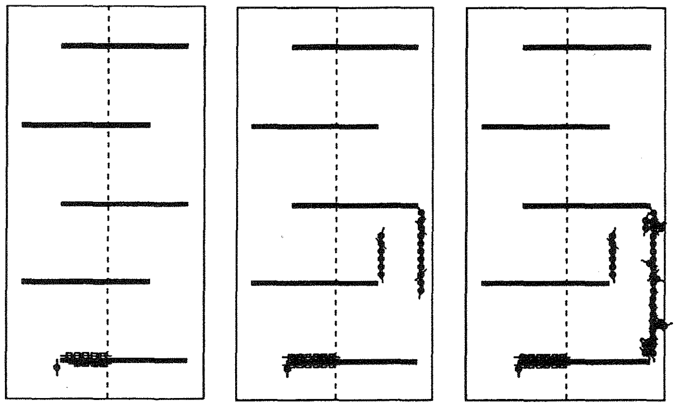

(a) 10th step (b) 30th step (c) 50th step

Fig.7. Internal failure pattern for stiff fiber
[●: Tensile failure; □: Shear failure]

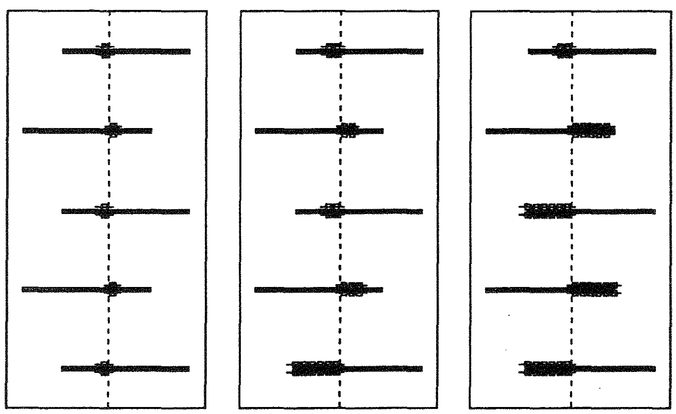

(a) 10th step (b) 30th step (c) 50th step

Fig.8. Internal failure pattern for soft fiber
[□: Shear failure]

The final failure mode is shown in Fig.7 and Fig.8. The gradual debonding along the interface between fiber and matrix is observed both for stiff fiber and for soft fiber as the shear lag model (see, e.g., Gopalaratnam and Shah(1987), Stang, Li and Shah(1990)) predicts. The debonding zone starts to extend from the fiber interface near the crack surface. Debonding is represented by shear failure, or the failure of the spring in the tangential direction at the element interface. It is observed that debonding occurs along the fiber with shorter embedded length. In case of soft fiber, the pullout process ends when debonding completes at all fibers crossing the crack surface. In case of stiff fiber, tensile failure occurs at the fiber end forming a tensile crack. The crack tends to extend in the direction perpendicular to the fiber. This tensile failure at the fiber end seems to occur due to the larger bond strength at the fiber-matrix interface.

The load-displacement curve is shown in Fig.9. The pullout force indicates the value for one fiber, while the displacement is the value at the crack surface. In case of stiff fiber, brittle and unstable behavior is observed because of the local tensile failure in the matrix. In case of soft fiber, gradual degradation after the peak pullout force is observed, indicating the gradual debonding along the fiber-matrix interface.

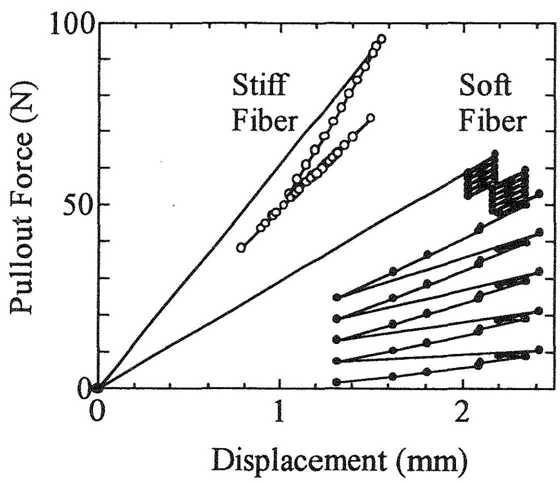


Fig.9. Pullout force-displacement relationship

## 4 Conclusion

A numerical simulation model using microstructural unit elements is presented for the analysis of the pullout behavior of fibers from the matrix of a fiber reinforced concrete. The appropriateness of the present model is confirmed through numerical simulations for a fiber reinforced concrete under tension. The use of the domain decomposition method is also shown for the case where the overall domain can be decomposed into subdomains.

## Acknowledgment

The support of the Grant-in-Aid for Scientific Research(C) of the Ministry of Education is gratefully acknowledged.

## References

Adeli, H. and Kamal, O.(1992) Concurrent analysis of large structures – I. Algorithms, II. Applications. **Computers and Structures**, 42(3), 413-424, 425-432.

Gopalaratnam, V.S. and Shah, S.P.(1987) Tensile failure of steel fiber-reinforced mortar. **Journal of Engrg. Mech.**, ASCE, 113(5), 635-652.

Li, V.C., Wang, Y. and Backer, S.(1991) A micromechanical model of tension-softening and bridging toughening of short random fiber reinforced brittle matrix composites. **Journal of Mech. Phys. Solids**, 39(5), 607-625.

Stang, H., Li, Z. and Shah, S.P.(1990) Pullout problem: stress versus fracture mechanical approach. **Journal of Engrg. Mech.**, ASCE, 116(10), 2136-2150.

Tsubaki, T.(1991) Deformation of concrete due to drying. **Proc., ASCE Engineering Mechanics Specialty Conference**, Mechanics Computing in 1990s and beyond, 2, 1149-1153.

Tsubaki, T.(1995) Numerical simulation of deformational properties of concrete by using microstructural unit elements. **Trans. of the Japan Concrete Institute**, 17, 119-126.

Tsubaki, T. and Sumitro, S.(1997) Modeling of tensile and shear mechanical properties of steel fiber reinforced concrete. **Concrete Research and Technology**, JCI, 8(1), 233-241.